



## RESEARCH ARTICLE

# Hyperacute autonomic and cortical function recovery following cardiac arrest resuscitation in a rodent model

Yu Guo<sup>1</sup> , Payam Gharibani<sup>2</sup>, Prachi Agarwal<sup>3</sup>, Sung-Min Cho<sup>4</sup>, Nitish V. Thakor<sup>1</sup> & Romergryko G. Geocadin<sup>4</sup> 

<sup>1</sup>Department of Biomedical Engineering, Johns Hopkins University School of Medicine, Baltimore, Maryland, USA

<sup>2</sup>Division of Neuroimmunology, Department of Neurology, Johns Hopkins University School of Medicine, Baltimore, Maryland, USA

<sup>3</sup>Department of Electrical and Computer Engineering, Johns Hopkins Whiting School of Engineering, Baltimore, Maryland, USA

<sup>4</sup>Departments of Neurology, Anesthesiology-Critical Care Medicine and Neurosurgery, Johns Hopkins University School of Medicine, Baltimore, Maryland, USA

## Correspondence

Romergryko G. Geocadin, Department of Neurology, Johns Hopkins University School of Medicine, 600 N Wolfe Street, Phipps 455, Baltimore, MD 21287, USA.  
Tel: +1(410)955-7481; Fax: +1(410)614-7903; E-mail: [rgeocad1@jhmi.edu](mailto:rgeocad1@jhmi.edu)

Received: 4 August 2023; Revised: 29 August 2023; Accepted: 11 September 2023

*Annals of Clinical and Translational Neurology* 2023; 10(12): 2223–2237

doi: 10.1002/acn3.51907

## Abstract

**Objective:** There is a complex interaction between nervous and cardiovascular systems, but sparse data exist on brain–heart electrophysiological responses to cardiac arrest resuscitation. Our aim was to investigate dynamic changes in autonomic and cortical function during hyperacute stage post-resuscitation. **Methods:** Ten rats were resuscitated from 7-min cardiac arrest, as indicators of autonomic response, heart rate (HR), and its variability (HRV) were measured. HR was monitored through continuous electrocardiography, while HRV was assessed via spectral analysis, whereby the ratio of low-/high-frequency (LF/HF) power indicates the balance between sympathetic/parasympathetic activities. Cortical response was evaluated by continuous electroencephalography and quantitative analysis. Parameters were quantified at 5-min intervals over the first-hour post-resuscitation. Neurological outcome was assessed by Neurological Deficit Score (NDS, range 0–80, higher = better outcomes) at 4-h post-resuscitation. **Results:** A significant increase in HR was noted over 15–30 min post-resuscitation ( $p < 0.01$  vs. 15-min, respectively) and correlated with higher NDS ( $rs = 0.56$ ,  $p < 0.01$ ). LF/HF ratio over 15–20 min was positively correlated with NDS ( $rs = 0.75$ ,  $p < 0.05$ ). Gamma band power surged over 15–30 min post-resuscitation ( $p < 0.05$  vs. 0–15 min, respectively), and gamma band fraction during this period was associated with NDS ( $rs \geq 0.70$ ,  $p < 0.05$ , respectively). Significant correlations were identified between increased HR and gamma band power during 15–30 min ( $rs \geq 0.83$ ,  $p < 0.01$ , respectively) and between gamma band fraction and LF/HF ratio over 15–20 min post-resuscitation ( $rs = 0.85$ ,  $p < 0.01$ ). **Interpretations:** Hyperacute recovery of autonomic and cortical function is associated with favorable functional outcomes. While this observation needs further validation, it presents a translational opportunity for better autonomic and neurologic monitoring during early periods post-resuscitation to develop novel interventions.

## Introduction

Cardiac arrest (CA) affects more than half a million people in the United States every year.<sup>1</sup> According to the “Heart Disease and Stroke Statistics—2023 Update” from the American Heart Association, only about 7.1% out-of-hospital CA patients may survive and achieve some functional recovery at hospital discharge.<sup>2</sup> Brain injury from

global cerebral ischemia induced by CA is the leading cause of high mortality and neurological disability in survivors.<sup>3</sup> However, merely around 10% of these deaths caused by CA meet the clinical criteria of brain death.<sup>4,5</sup> Most deaths related to CA-induced brain damage are due to active withdrawal of life-sustaining treatment as the result of a prediction of poor neurological outcome.<sup>6</sup> For this reason, accurate neurological prognostication plays a

critical role in postarrest care for comatose patients since it helps clinicians to make the decision of continuing futile treatments for patients in whom poor outcomes are inevitable or ending life supports for those who do not have a chance to achieve a neurological recovery.<sup>6</sup> The current prognostic approach uses a multivariable model based on the clinical status of the patient together with ancillary testing, including neurophysiology (such as electroencephalography, EEG), biochemical markers, and neuroimaging.<sup>6</sup>

It was shown that neuronal damage can appear in minutes after CA,<sup>7</sup> resulting in selective regional damage in various brain areas.<sup>8</sup> The most vulnerable area is the cerebral cortex, followed by several subcortical structures, including the thalamus, hippocampus, and striatum.<sup>6–8</sup> In contrast, the brainstem has a lesser vulnerability.<sup>6,9,10</sup> EEG is the recording of cortical neuronal activity and has been studied in translational animal models to prognosticate neurological outcomes post-CA resuscitation. Clinical reports reveal multiple malignant EEG features,<sup>11,12</sup> such as burst-suppression pattern,<sup>13</sup> low voltage,<sup>14</sup> and identical bursts,<sup>15</sup> which may correlate with poor outcomes. Previously, we found that increased EEG bursting during the first 10–30 min after resuscitation was linked to favorable neurological outcomes in an asphyxial CA (ACA) rodent model.<sup>16</sup> Using quantitative EEG analysis, we uncovered that ACA-induced brain injury led to a significant decrease in EEG entropy, while a good neurological recovery manifested a rapid return to a higher entropy value.<sup>17</sup>

Heart rate variability (HRV) has been employed to quantify autonomic activity<sup>18</sup> and is considered evidence of brainstem integrity.<sup>19</sup> Relative to other regions of the brain, the brainstem has lesser vulnerability to hypoxia.<sup>6,9,10</sup> It is highly possible that once dysfunction of the brainstem occurs, it reflects more severe brain damage. In prior work, we found that short-term HRV was a sensitive marker for indicating the onset of asphyxia in our rodent model of ACA.<sup>20</sup> Clinical studies identified that low HRV was inversely related to mortality in critically ill patients.<sup>21,22</sup> Moreover, it was reported that a relative decrease in sympathetic tone, represented by decreased low-frequency power in HRV measures, during the very early stage (30–60 min) after the return of spontaneous circulation (ROSC) was associated with a higher 24-h mortality in out-of-hospital CA patients.<sup>23</sup>

There is a complex interaction between the nervous and cardiovascular systems.<sup>10</sup> Many studies have focused separately on cortical or autonomic injury, but the dysfunction in one system may result in functional alterations in another. The aim of this study was to utilize our ACA rodent model and investigate the early responses of the cardiac and cortical electrophysiological activity as

well as a potential interaction between these two after resuscitation in relation to acute behavioral recovery. Here, we hypothesize that an early recovery of brain–heart electrical activity during the hyperacute stage of post-CA resuscitation would be linked to favorable acute neurological outcomes.

## Methods

This study was approved by the Johns Hopkins Medical Institute Animal Care and Use Committee. All procedures involved were conducted in accordance with the National Institutes of Health guide and reported based on the ARRIVE guidelines (<https://www.nc3rs.org.uk/arrive-guidelines>). For this research, we employed an ACA rat model that has been well-defined by our laboratory and others.<sup>16,24–26</sup> The sample size calculation and power analysis were extrapolated from our prior work. Based on the result of Neurological Deficit Score (NDS) as the primary outcome, assuming  $\alpha = 0.05$  with a power of 0.80 and a difference of mean NDS between the two groups was 15, the minimum sample size per group was five subjects. Ten adult Wistar male rats (400–450 g; 11–12 weeks old; Charles River, Wilmington, MA) were subjected to 7-min ACA. Our prior study disclosed that a minimum of five rats (male) per group was adequate to detect the difference in brain injury induced by our ACA model.<sup>25,27</sup> All animals were pair-housed in a quiet environment with 12-h day/night cycles and free access to food and water.

## Experimental preparations, asphyxial CA, and resuscitation

The animals were anesthetized with isoflurane (4% for induction and 1.6–1.8% for maintenance carried by 50%:50% nitrogen and oxygen mixed gas at 4 L/min) and intubated with a 16G catheter. Following the intubation, the animals were positioned on a stereotactic frame (Kopf Instruments, Tujunga, CA) under 1.6–1.8% isoflurane via a nose cone. The usage of a nose cone at this stage was because the teeth bar of the stereotactic frame was not compatible with the ventilator connector. Therefore, we used the nose cone to deliver isoflurane while the animals were on the stereotactic frame for the placement of EEG electrodes. For a limited time on the nose cone, the animals were implanted with three epidural screw electrodes (Plastics One Inc., Roanoke, VA). Two frontal electrodes were implanted 2 mm anterior and 2 mm lateral to bregma (right: channel A; left: channel B) with a third ground/reference electrode located at 2 mm posterior to lambda. After the electrode implantation, the animals were taken off the nose cone and connected to a mechanical ventilator (Kent Scientific, Torrington, CT) with 1.6–1.8%

isoflurane for the rest of the experiment. The ventilation settings were maintained with a tidal volume of 10 mL/kg and a positive expiratory end pressure of 3 cm H<sub>2</sub>O at a respiration rate of approximately 50 breaths/min. Cannulation of the femoral artery and vein was performed on the animals afterward. Following this, the EEG electrodes were connected to an RX5 TDT device (Tucker-Davis Technologies, Alachua, FL) for EEG recording. Mean arterial pressure (MAP) and electrocardiography (ECG) were monitored continuously through the same device. A heating pad was used to keep the animals' body temperature (BT) at 36–37°C during the surgery. Arterial blood gas (ABG) was measured at baseline, 15-min post-ROSC, and end of recordings by using an i-STAT analyzer (Abbott Point of Care Inc., Princeton, NJ).

After a 5-min period of baseline recording, the ACA procedure started with a 5-min washout period: 2-min of 100% pure oxygen without isoflurane followed by injecting Rocuronium Bromide (2 mg/kg, I.V.) and then 3-min of 20% pure oxygen mixed with 80% nitrogen (room air). Global asphyxia was induced by stopping the mechanical ventilation for 7 min. The achievement of CA was defined as MAP <10 mmHg with a nonpulsatile-pressure wave. Cardiopulmonary resuscitation (CPR) was initiated by restarting the mechanical ventilation with 100% oxygen at a respiration rate of 80 breaths/min, administering epinephrine (7 µg/kg, I.V.) and NaHCO<sub>3</sub> (1 mmol/kg, I.V.), and applying sternal chest compressions with two fingers (~200 compressions/min). The achievement of ROSC was defined by MAP >50 mmHg within 2-min CPR. Following successful resuscitation, the animals were hyperventilated for about 20 min, and then, the respiration rate was adjusted to maintain PaCO<sub>2</sub> at 35–45 mmHg. It is worth mentioning that epinephrine was only applied once during the CPR procedure and was not administrated to the animals during post-ROSC EEG and ECG recording. For this experiment, the heating pad was removed when the baseline recording started, but the BT was monitored through a rectal temperature probe throughout the experiment. BT was allowed to progress spontaneously as it provides valuable information on the autonomic responses to varied conditions. BT may influence HR dynamics as well. Hence, the heating pad was removed to allow us to observe BT under an uncontrolled condition and assess its relationship with the HR changes after resuscitation.

### ECG recording and HRV analysis

To limit interference from the local electrical environment, 59–61 Hz frequency was filtered out of ECG recordings using a second-order Butterworth notch filter fit to the final target sample rate of 939 Hz. The R peaks were automatically detected by an adaptive threshold. The

time intervals between two successive R peaks were determined as RR intervals. Power spectral density was utilized for HRV analysis.<sup>28</sup> A Fast Fourier Transform-based Welch's periodogram approach was implemented to obtain the power spectral density. For calculations of Welch's periodogram, a Hann window with 50% overlap was applied to the input RR interpolated at 10 Hz. The frequency bands of interest in HRV analysis were very low frequency (VLF, 0–0.04 Hz), low frequency (LF, 0.04–0.15 Hz), and high frequency (HF, 0.15–0.4 Hz). The frequency-domain measurements extracted from the power spectral density estimate for each frequency band included the relative power of VLF, LF, and HF components. The LF and HF components were converted to normalized units by dividing their respective magnitudes by total power, leaving out the VLF power. LF power is considered a measure of sympathetic activity, while HF power is a measure of parasympathetic activity.<sup>29</sup>

### EEG recording and quantitative EEG analysis

The raw EEG was filtered with a second-order Butterworth notch filter for the range of 59–61 Hz. The digitized EEG was then downsampled by a power of 50 to a target sample rate of 244 Hz. The detrended standard deviation of the downsampled EEG was calculated to determine approximate bin thresholding for the calculation of Shannon entropy. The downsampled EEG was divided into nonoverlapping eight-second windows and decomposed into frequency bands using a one-dimensional, five-level dyadic, symlet9 wavelet decomposition, which after coefficient-based reconstruction provides six signals representing the target ranges of supergamma as 61.5–122 Hz, gamma as 30.75–61.5 Hz, beta as 15.375–30.75 Hz, alpha as 7.688–15.375 Hz, theta as 3.844–7.688 Hz, and delta as 1.922–3.844 Hz.<sup>30</sup> The spectral power of each range was calculated from the wavelet coefficients using the Parseval equivalence identity. The total spectral power of all ranges was used as the denominator in calculating the power fraction. Power calculations were made at 5-min intervals starting from the ROSC point. Shannon entropy was calculated at the same intervals for the full frequency range using a bin-counting algorithm aligned by the earlier-determined detrended standard deviation thresholds as range cutoffs. Entropy has been used to quantify the randomness of EEG signals to reflect their complexity and is defined as<sup>31,32</sup>

$$S = - \sum_{i=1}^L p_i \ln p_i$$

where  $p_i$  is the probability that the signal belongs to a considered amplitude interval with  $L$  partitions and with

the understanding that (a)  $\sum_{i=1}^L p_i = 1$  with  $0 \leq p_i \leq 1, i = 1, \dots, L$  and (b)  $p_i \ln p_i = 0$  if  $p_i = 0$ . These methods used in quantitative EEG analysis were validated in our previous research.<sup>30,33–35</sup>

For this study, post-resuscitation recording was up to 90 min, and isoflurane was not applied to the CA-subjected animals during this recording period, and the animals were allowed to recover spontaneously. In our prior work, animals subjected to 7-min CA remained comatose status over the first 2–3 h after resuscitation.<sup>25,27</sup> Hence, to minimize the potential influence of isoflurane on the recovery of cortical and cardiac electrical activity, we did not use isoflurane during the recording period and also did not observe the CA-subjected animals regain awareness over this duration. At the end of the recording, the animals were extubated. All catheters were removed, and incisions were closed with 4–0 sutures. The animals were allowed to recover in a dim and quiet environment.

### Neurological outcome evaluation

The NDS has been widely used for neurological outcome evaluation in this ACA rodent model.<sup>26,33,34,36</sup> The NDS ranges from 0 (brain death) to 80 (healthy animal) and was assessed by two experienced observers at 4-h post-ROSC (see Table S1). We chose the 4-h after resuscitation as the desired time point for evaluating neurological outcomes in this study since our focus was to study the postischemia recovery in the hyperacute period when the brain is still most likely receptive to potential therapies.<sup>37</sup> Based on our previous study, we used the score of 60 as the threshold to differentiate favorable and unfavorable neurological outcomes.<sup>16</sup> Accordingly, the CA-subjected animals were separated into two groups, namely the poor (NDS < 60) and good outcome groups (NDS ≥ 60;  $n = 5$  per group), with poor and good neurological outcomes, respectively, for further analysis and interpretation of the cortical EEG and cardiac HRV responses. After the NDS evaluation, the CA-subjected animals were humanly sacrificed.

### Statistical analysis

Data were analyzed by SPSS 26.0 version (SPSS Inc., Chicago, IL) and Graph Pad Prism 9.2.0 version (Graph Pad, San Diego, CA). Kolmogorov–Smirnov test was used for the normality test. An unpaired t-test (including Welch's correction) was chosen for comparisons between the two groups. Regarding comparisons among multiple groups, one-way or two-way ANOVA (including repeated measures) was performed along with Bonferroni's correction. Spearman's rank correlation was applied to assess correlations between different parameters. The trapezoidal rule was utilized for the

calculation of the area under the curve (AUC). The data were presented as mean ± standard deviation (SD). The statistical significance threshold was set at  $p \leq 0.05$ .

## Results

### Neurological deficit outcome after cardiac arrest resuscitation

A total of 10 CA-subjected male rats completed the experimental protocol (Fig. 1). The time to CA was  $251.10 \pm 23.86$  sec, and the time to ROSC was  $62.70 \pm 17.56$  sec. With our focus on the hyperacute post-resuscitation period, post-CA neurological deficits were evaluated by NDS at 4-h post-ROSC, and the NDS results ranged from 52 to 73 ( $62.70 \pm 7.96$ ,  $n = 10$ ). Based on the NDS score of 60 as the cutoff,<sup>16</sup> the CA-subjected animals were divided into the poor outcome group (NDS < 60) and the good outcome group (NDS ≥ 60). There was no significant difference between the two groups in body weight, preparation time, time to CA, time to ROSC, and ABG parameters (including pH, PaCO<sub>2</sub>, SaO<sub>2</sub>, and HCO<sub>3</sub><sup>−</sup>) at baseline, 15-min post-ROSC and end of the recording ( $p > 0.05$ ), except for the pH value measured at the end of the recording ( $p = 0.04$ ; Table 1).

### Acute cardiac rhythm response to cardiac arrest resuscitation

Following resuscitation, a significant increase in heart rate (HR) was noted from 15- to 30-min post-ROSC ( $p < 0.001$  vs. 15-min, respectively;  $n = 10$ ) with a peak at 30-min ( $473.80 \pm 40.21$  beats/min for 30-min vs.  $355.00 \pm 25.41$  beats/min for 15-min,  $p < 0.001$ ; Fig. 2A). The normal range of HR changes in rats is around 250–500 beats/min.<sup>38</sup> The relative increase of HR (compared to 15-min post-ROSC) was significantly higher in the good outcome group at 25-min post-ROSC when compared to the poor outcome group ( $126.00 \pm 35.79$  beats/min vs.  $72.60 \pm 34.62$  beats/min,  $p = 0.04$ ;  $n = 5$  per group; Fig. 2B). Meanwhile, the AUC of increased HR (relative to HR at 15-min post-ROSC) over 20–30 min following resuscitation in the poor outcome group was remarkably lower in animals with good NDS results ( $693.00 \pm 322.28$  vs.  $1149.50 \pm 307.69$ ,  $p \leq 0.05$ ; Fig. 2C). We also found a moderate positive correlation between increased HR (relative to HR at 15-min post-ROSC) over 20–30 min post-ROSC with higher NDS ( $r_s = 0.559$ ,  $p = 0.001$ ; Fig. 2D). Moreover, the increased HR (relative to 15-min post-ROSC) at 20-, 25-, and 30-min post-ROSC showed strong correlations with better NDS, respectively ( $r_s = 0.671$ ,  $p = 0.04$ ;  $r_s = 0.814$ ,  $p = 0.006$ ;  $r_s = 0.760$ ,  $p = 0.001$ , respectively; Fig. 2E).

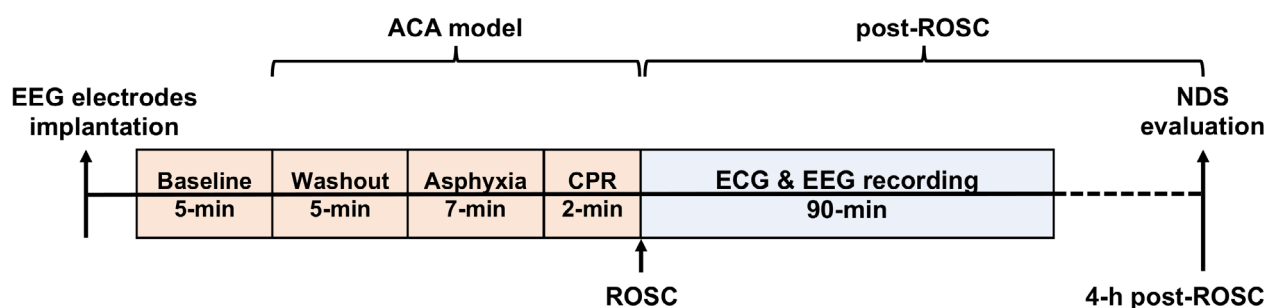


**Figure 1.** Schematic diagram of experimental design. ACA, asphyxial cardiac arrest; ECG, electrocardiography; EEG, electroencephalography; NDS, neurological deficit score; ROSC, return of spontaneous circulation.

**Table 1.** Prearrest baseline and arrest-resuscitation variables between poor and good outcome groups.

Parameters	Poor outcome (n = 5)	Good outcome (n = 5)	p value
Body weight (g)	416.2 ± 24.2	421.6 ± 20.0	0.71
Preparation time (min)	172.8 ± 14.7	161.4 ± 7.8	0.16
Time to CA (sec)	241.8 ± 24.1	260.4 ± 22.0	0.23
Time to ROSC (sec)	68.2 ± 20.9	57.2 ± 13.5	0.35
Baseline ABG			
pH	7.432 ± 0.030	7.440 ± 0.053	0.79
PaCO <sub>2</sub> (mmHg)	43.84 ± 4.22	43.28 ± 5.17	0.86
SaO <sub>2</sub> (%)	99.6 ± 0.5	99.6 ± 0.5	1
HCO <sub>3</sub> <sup>-</sup> (mmol/L)	27.14 ± 4.37	29.26 ± 1.40	0.33
15-min post-ROSC ABG			
pH	7.371 ± 0.045	7.325 ± 0.099	0.37
PaCO <sub>2</sub> (mmHg)	47.18 ± 4.50	56.20 ± 9.71	0.10
SaO <sub>2</sub> (%)	100	100	–
HCO <sub>3</sub> <sup>-</sup> (mmol/L)	27.28 ± 0.91	29.10 ± 2.10	0.11
End of recording ABG			
pH	7.447 ± 0.035	7.424 ± 0.018	0.04
PaCO <sub>2</sub> (mmHg)	42.16 ± 3.96	42.96 ± 3.72	0.53
SaO <sub>2</sub> (%)	100	100	–
HCO <sub>3</sub> <sup>-</sup> (mmol/L)	29.07 ± 0.89	28.12 ± 2.76	0.21

Data presented as mean ± SD. Unpaired *t*-test (including with Welch's correction) was used for comparisons between poor and good outcome groups.

ABG, arterial blood gas; CA, cardiac arrest; NDS, neurological deficit score; ROSC, return of spontaneous circulation.

The first hour after resuscitation is the most remarkable, with significant fluctuations in cardiac rhythm, MAP, and neurological signals recovery. An elevation of MAP was noted around 10-min post-ROSC, but this dynamic pattern was different from the changes in HR (Fig. S1). Also, no differences in MAP changes were noted between the good and poor outcome groups over 15–30 min post-ROSC. We found no correlations between MAP and NDS over this period ( $p > 0.05$ , respectively). Epinephrine, with an elimination half-life of 11 min,<sup>39</sup> was only administered during CPR, and repeat dosing was not done afterward.

### Autonomic response to cardiac arrest resuscitation

The autonomic response can be inferred from the variability in the cardiac rhythm. We investigated the heart rate fluctuation accompanying the increase in HR over 15–30 min post-ROSC. HRV was assessed by spectral analysis of the heart rate intervals (RR intervals) derived from ECG recordings at 5-min segmentations. Our results revealed that LF power and LF/HF ratio of the good outcome group trended higher, though not statistically significant, than the poor outcome group during this period, especially at 15–20 min post-ROSC (LF power:  $0.37 \pm 0.15$  vs.  $0.20 \pm 0.06$ ; LF/HF ratio:  $0.41 \pm 0.34$  vs.  $0.18 \pm 0.10$ ;  $p > 0.05$ , respectively), while HF power trended lower in the good outcome group ( $0.78 \pm 0.12$  vs.  $0.85 \pm 0.07$ ,  $p > 0.05$ ; Fig. 3A). Over 15–20 min post-ROSC, both LF power and LF/HF ratio were positively correlated with higher NDS ( $r_s = 0.600$ ,  $p = 0.074$  and  $r_s = 0.749$ ,  $p = 0.046$ , respectively; Fig. 3B), possibly due to enhanced sympathetic tone during the very acute stage after resuscitation, which correlated better acute neurological outcome.

### Body temperature changes following cardiac arrest resuscitation

Body temperature (BT) changes are also influenced by autonomic function. During 15- to 30-min post-ROSC, there was a significant increase of BT, ranging from  $35.57 \pm 0.75$  to  $37.84 \pm 0.56$  °C, in CA-subjected animals (vs. 15-min:  $p < 0.05$ , respectively; Fig. S2), but this trend peaked around 60-min post-ROSC ( $38.84 \pm 0.55$  °C). No significant differences in BT changes were noted between the good outcome and poor outcome groups over this period ( $p > 0.05$ , respectively). On the contrary, increased BT may be related to elevated HR. We found a weak association between BT changes and increased HR



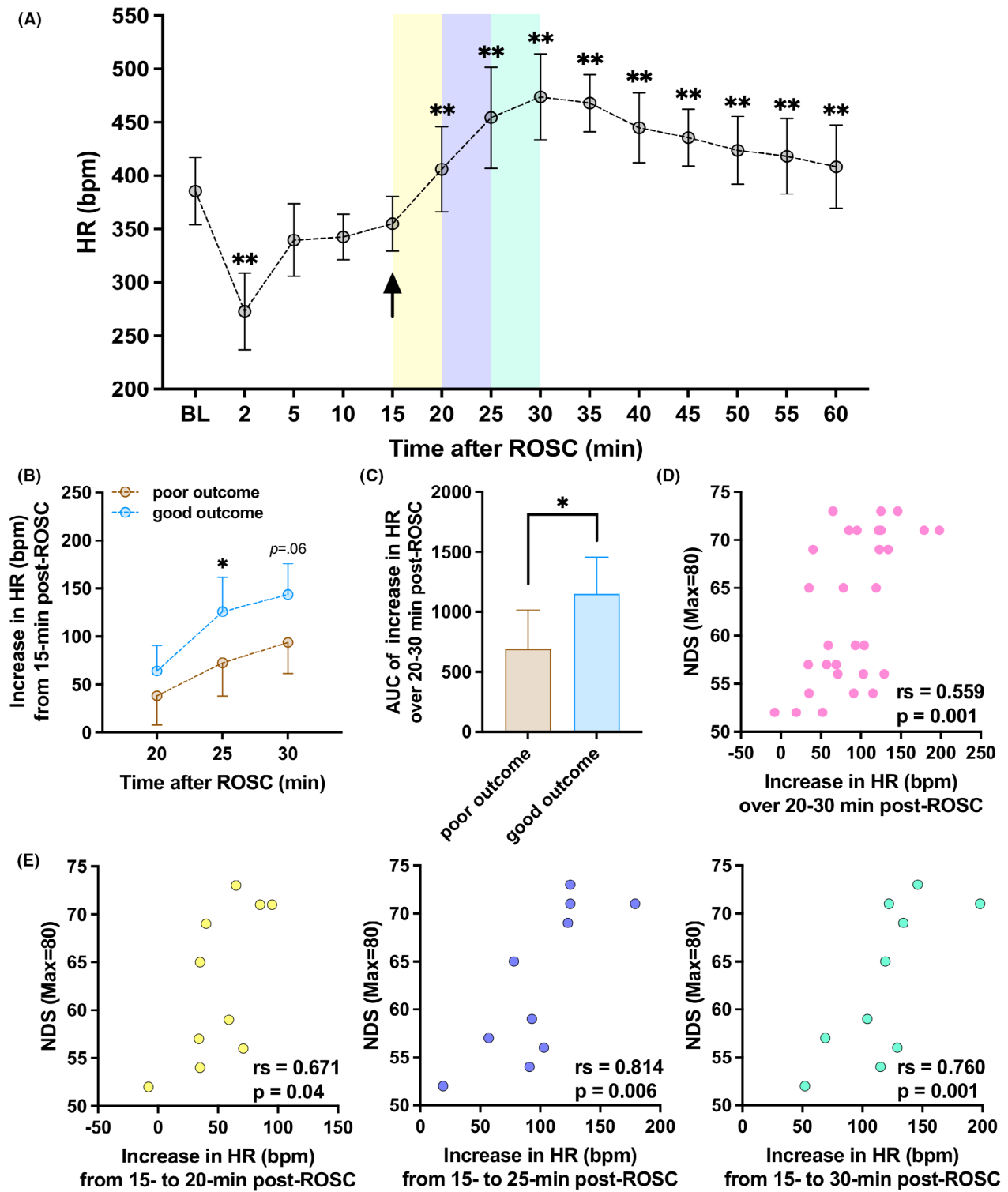


**Figure 2.** HR dynamics following resuscitation in ACA rats and its correlation with neurological outcomes. (A) HR elevated remarkably from 15- to 30-min post-ROSC ( $p < 0.001$  vs. 15-min, respectively;  $n = 10$ ). (B) The increase in HR at 25-min from 15-min post-ROSC was significantly higher in animals with good NDS results than that in the poor outcome group ( $p = 0.04$ ;  $n = 5$  per group). (C) The AUC of increased HR (from 15-min post-ROSC) over 20–30 min post-ROSC was significantly higher in the good outcome group as compared with the poor outcome group ( $p \leq 0.05$ ). (D) The changes in HR over 20–30 min from 15-min post-ROSC were positively correlated with NDS ( $r_s = 0.559$ ,  $p = 0.001$ ). (E) The increased HR at 20-, 25-, and 30-min from 15-min post-ROSC was strongly correlated with higher NDS, respectively ( $r_s = 0.671$ ,  $p = 0.04$ ;  $r_s = 0.814$ ,  $p = 0.006$ ;  $r_s = 0.760$ ,  $p = 0.001$ , respectively). ACA, asphyxial cardiac arrest; AUC, the area under the curve; BL, baseline; bpm, beats per minute; HR, heart rate; NDS, neurological deficit score; ROSC, return of spontaneous circulation. Data represent as mean  $\pm$  SD. Comparisons among HR temporal changes were performed with repeated measures one-way ANOVA with Bonferroni correction; comparisons between poor and good outcome groups in HR changes were conducted via repeated measures two-way ANOVA with Bonferroni correction; correlations between HR and NDS were performed with Spearman's correlation. \* $p \leq 0.05$ , \*\* $p < 0.001$ .

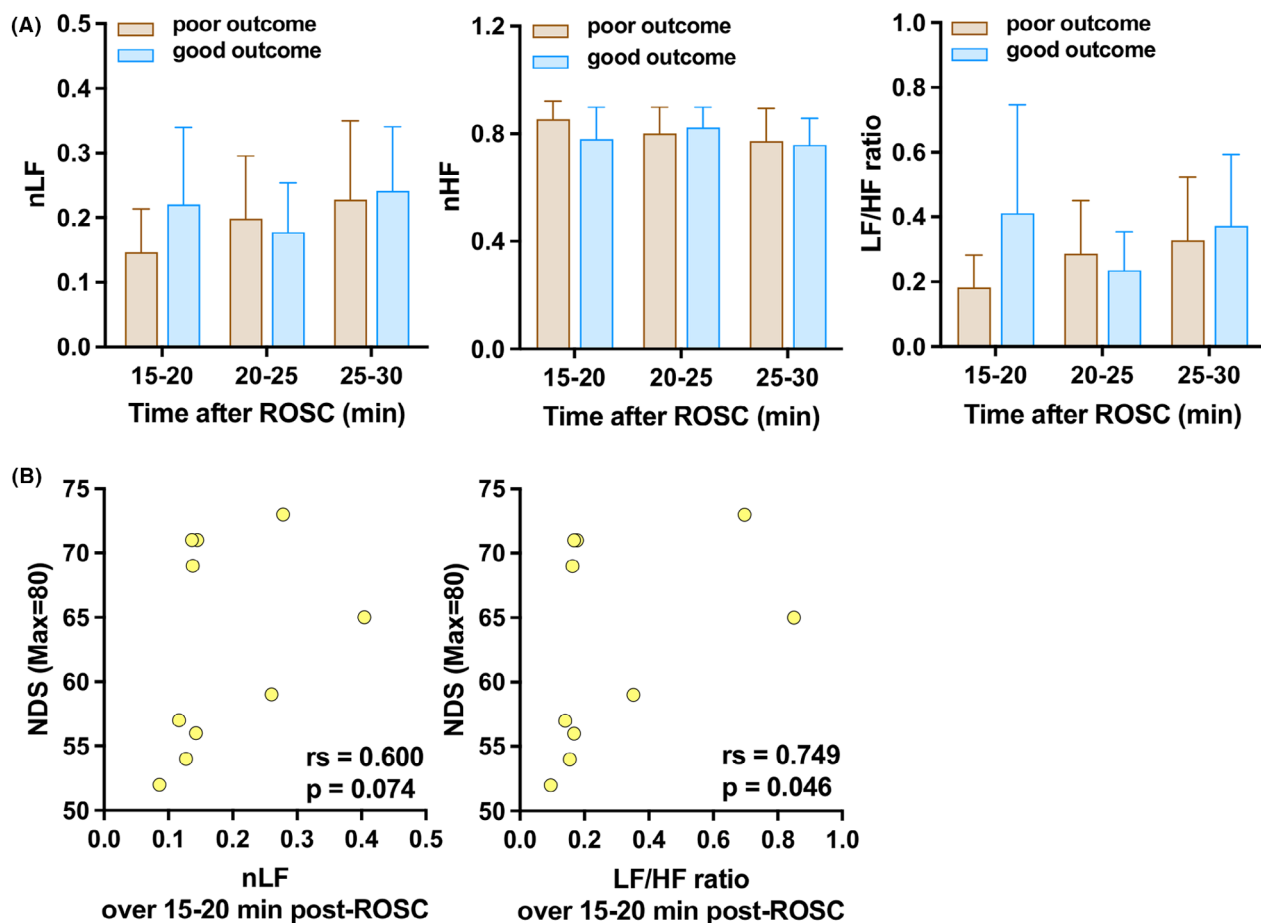


**Figure 3.** HRV analysis following resuscitation in ACA rats and its correlation with neurological outcomes. (A) Normalized LF power and LF/HF ratio over 15–30 min post-ROSC were relatively elevated in the good outcome group as compared with the poor outcome group, especially over 15–20 min post-ROSC ( $p > 0.05$ , respectively;  $n = 5$  per group). (B) The increase of normalized LF power and LF/HF ratio during 15–20 min post-ROSC was positively associated with higher NDS ( $r_s = 0.600$ ,  $p = 0.074$ ;  $r_s = 0.749$ ,  $p = 0.046$ , respectively). ACA, asphyxial cardiac arrest; NDS, neurological deficit score; nHF, normalized high frequency; nLF, normalized low frequency; ROSC, return of spontaneous circulation. Data represent as mean  $\pm$  SD. Comparisons between poor and good outcome groups in nLF, nHF, and LF/HF ratio were conducted by repeated measures two-way ANOVA with Bonferroni correction; correlations between HRV parameters and NDS were performed with Spearman's correlation.

(relative to HR at 15-min post-ROSC) over 15–30 min post-ROSC ( $r_s = 0.268$ ,  $p > 0.05$ ).

### Cortical neuronal dynamics following resuscitation

The dynamic changes of cortical neuronal activity were assessed by quantitative EEG analysis. As shown in (Fig. 4A), there was a significant elevation in total power

over 15–30 min post-ROSC ( $p < 0.01$  vs. 0–5, 5–10, and 10–15 min, respectively). Among the six EEG subbands (including delta, theta, alpha, beta, gamma, and super-gamma), beta, gamma, and super-gamma band power exhibited significant increases over 15–30 min post-ROSC ( $p < 0.05$  vs. 0–5, 5–10, and 10–15 min, respectively) and reached the peaks at 20–25 min during the first-hour post-ROSC ( $p \leq 0.05$  vs. 30–35, 35–40, 40–45, 45–50, 50–55, and 55–60 min, respectively). In our prior work, we

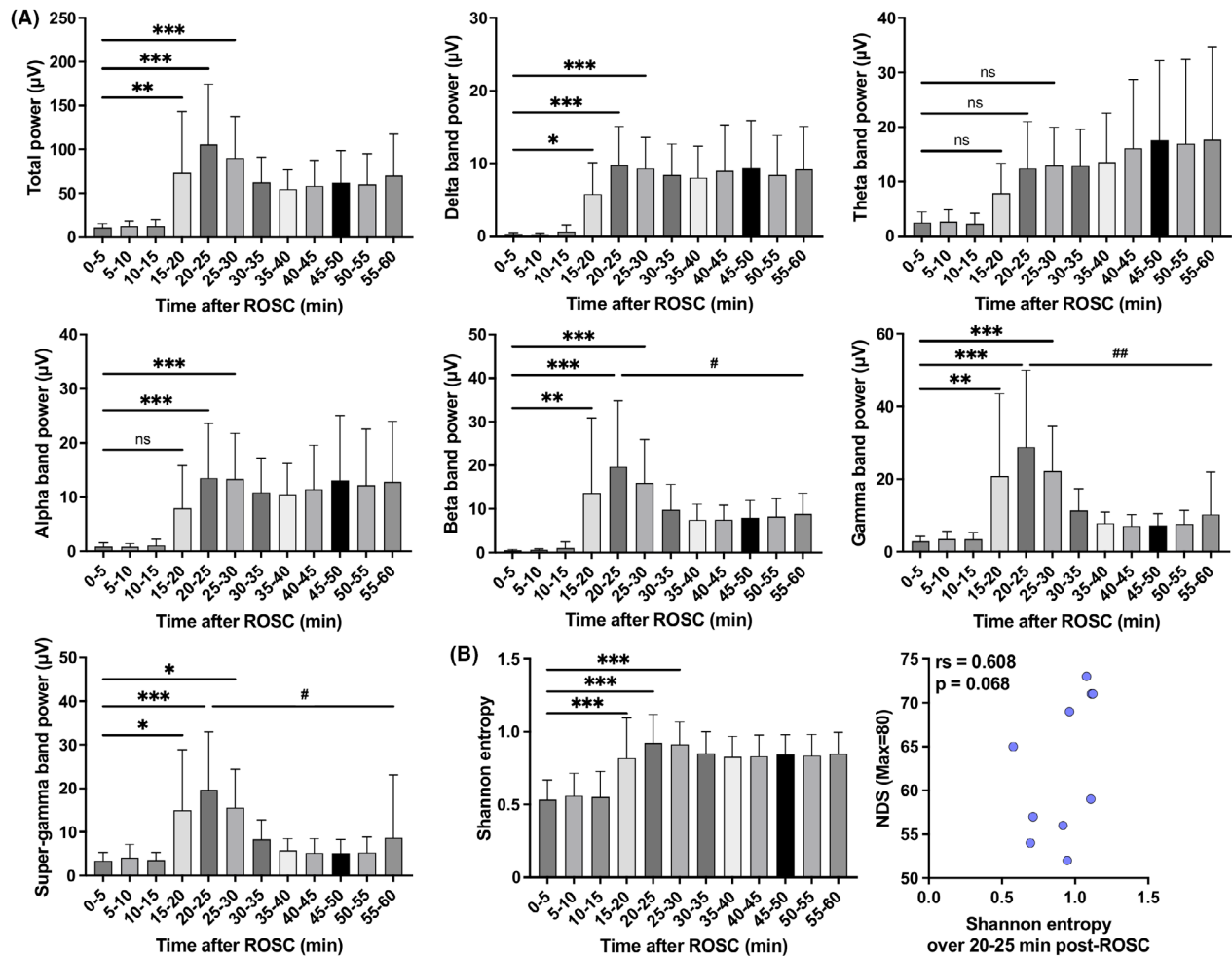


**Figure 4.** EEG changes following resuscitation in ACA rats and its correlation with neurological outcomes. (A) Total power over 15–30 min post-ROSC was increased significantly in comparison with the first 15 min post-resuscitation (vs. 0–5, 5–10, and 10–15 min,  $p < 0.01$ , respectively;  $n = 10$ ). Among six EEG subbands, beta, gamma, and super-gamma band power exhibited significant increases over 15–30 min post-ROSC ( $p < 0.05$  vs. 0–5, 5–10, and 10–15 min, respectively) and reached the peaks at 20–25 min during the first-hour post-ROSC ( $p \leq 0.05$  vs. 30–35, 35–40, 40–45, 45–50, 50–55, and 55–60 min, respectively). (B) Shannon entropy manifested an increase during 15–30 min post-resuscitation ( $p < 0.001$  vs. 0–5, 5–10, and 10–15 min,  $p < 0.01$ , respectively). Shannon entropy over 20–25 min post-ROSC was correlated positively with NDS, though statistical significance was not found ( $r_s = 0.608$ ,  $p = 0.068$ ). ACA, asphyxial cardiac arrest; EEG, electroencephalography; NDS, neurological deficit score; ROSC, return of spontaneous circulation. Data represent as mean  $\pm$  SD. Comparisons among temporal changes of EEG parameters were performed with repeated measures one-way ANOVA with Bonferroni correction; correlations between EEG parameters and NDS were performed with Spearman's correlation. \* vs. 0–5, 5–10, 10–15 min, respectively,  $p < 0.05$ ; \*\* vs. 0–5, 5–10, 10–15 min, respectively,  $p < 0.01$ ; \*\*\* vs. 0–5, 5–10, 10–15 min, respectively,  $p < 0.001$ ; # vs. 30–35, 35–40, 40–45, 45–50, 50–55, 55–60 min, respectively,  $p < 0.05$ ; ## vs. 30–35, 35–40, 40–45, 45–50, 50–55, 55–60 min, respectively,  $p < 0.01$ .



have developed the mathematic method of using entropy to quantify the complexity of EEG signals, and the higher entropy indicates more vigorous neurological activity.<sup>31,32</sup> Here, we found that Shannon entropy values calculated from the EEG signals demonstrated a noticeable increase during 15–30 min post-ROSC ( $p < 0.001$  vs. 0–5, 5–10, and 10–15 min, respectively), and Shannon entropy values over 20–25 min post-ROSC were correlated positively with NDS, though not statistically significant ( $r_s = 0.608$ ,  $p = 0.068$ ; Fig. 4B).

Regarding EEG subband power fraction over 15–30 min post-ROSC, it was shown in (Fig. 5A) that gamma band fractions were significantly higher than the other subbands (including delta, theta, alpha, and beta band fraction) ( $p < 0.05$ , respectively), indicating that the gamma band power was the dominant power over 15–30 min post-ROSC. We found strong and positive correlations between gamma band power over 15–30 min post-ROSC and higher NDS ( $r_s = 0.705$ ,  $p = 0.027$ ,  $r_s = 0.693$ ,  $p = 0.031$ , and  $r_s = 0.614$ ,  $p = 0.064$ , respectively; Fig. 5B) and between gamma band fraction during the same period and better neurological outcomes ( $r_s = 0.796$ ,  $p = 0.008$ ,  $r_s = 0.912$ ,  $p < 0.001$ , and  $r_s = 0.669$ ,  $p = 0.04$ , respectively; Fig. 5C).

### Changes in cardiac rhythm response are correlated with cortical neuronal activity

Significant increases in HR and gamma band power were observed in CA-subjected animals during 15–30 min post-ROSC. To study the relationship between cardiac rhythm changes and cortical neuronal dynamics after resuscitation, Spearman's correlations were performed between increased HR/HRV parameters and EEG signals. Very strong correlations were identified between increased HR and gamma band power at 15–20 min ( $r_s = 0.827$ ,  $p = 0.005$ ), 20–25 min ( $r_s = 0.912$ ,  $p < 0.001$ ), and 25–30 min ( $r_s = 0.891$ ,  $p = 0.001$ ) post-ROSC, respectively (see Fig. 6A). Moreover, gamma band fraction over 15–20 min post-ROSC exhibited significantly positive correlations with LF power ( $r_s = 0.770$ ,  $p = 0.013$ ) as well as LF/HF ratio ( $r_s = 0.846$ ,  $p = 0.003$ ) over the same period (Fig. 6B).

### Discussion

Our study demonstrates dysfunction of both cardiac rhythms (as reflected in the HR changes) and cortical neuronal activities (as reflected in the EEG signals) after CA. These dual findings imply disturbed brain–heart coupling. Our observation of the hyperacute recovery pattern shows an early recovery of the brain–heart axis, including

the concurrent surge in both EEG signal band powers and sympathetic tone, is associated positively with a better neurological functional outcome. Further, this transient sympathetic activation (shown as increased HR and elevated sympathetic tone) is concurrent and correlated with enhanced cortical arousal (shown as surged gamma band activity).

In this study, we observed significant augmentation in both EEG total power and entropy over 15–30 min post-ROSC as compared with the first 15 min after resuscitation, suggesting there is a remarkable increase in cortical neuronal activity and its complex recovery during this period. Interestingly, we found that gamma band power peaked during the same period and was the dominant power among the subbands. Also, higher gamma band power and fraction over 15–30 min post-ROSC had strong and positive correlations with higher NDS. EEG gamma band oscillations are linked closely to enhanced cortical arousal.<sup>40,41</sup> Our findings exhibit that an early recovery of EEG activity, shown as higher entropy values that indicate more vigorous neurological activity and stronger gamma band activity that relates to enhanced cortical arousal status during the hyperacute stage after resuscitation, is correlated with favorable acute neurological outcome.

Coma is defined as a failure of both arousal and complete unresponsiveness to external or internal stimuli.<sup>42</sup> The EEG has been used to prognosticate neurological outcomes after CA.<sup>43</sup> Persistent generalized burst suppression in post-CA patients is correlated with poor neurological recovery.<sup>44</sup> In prior work in CA-subjected rats, we reported that flat EEG underwent increasing EEG bursting during the first 10–30 min post-ROSC that evolved to continuous EEG activity, resulting in favorable neurological outcomes.<sup>16</sup> Entropy, as a mathematical measure of randomness of EEG patterns, has been utilized to monitor injury and recovery since lower entropy values were seen in pathological EEG patterns after CA.<sup>32,45</sup> Using subband entropy of EEG, we also uncovered that in rats subjected to 7-min ACA, continuous EEG activity began to return at approximately 15–20 min after resuscitation.<sup>46</sup> In this present study, we found EEG activity (represented by entropy as well as gamma band power) surged over 15–30 min post-ROSC, and this recovery of EEG activity is linked to better neurological outcomes. These results are consistent with our previous findings.

Arousal requires intact subcortical and brainstem function, and without arousal, it is not possible to regain awareness.<sup>42</sup> The ascending reticular activating system (ARAS), which is derived from the brainstem, has been recognized as the primary region in modulating arousal.<sup>47</sup> Gamma band oscillations are considered a brain-wide property of the awake brain.<sup>48</sup> It has been suggested that

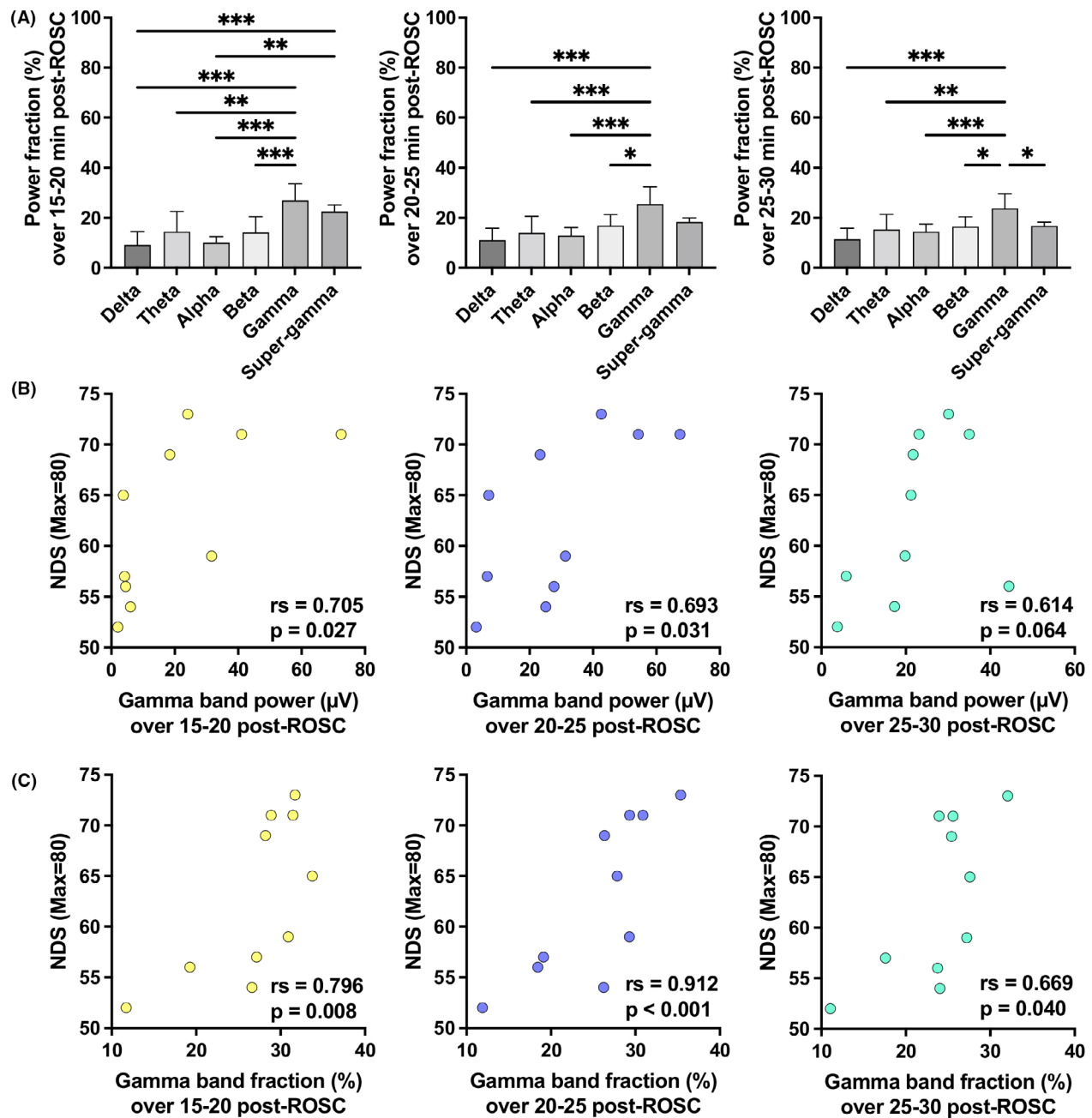


**Figure 5.** EEG subband power fraction over 15–30 min following resuscitation and its correlation with neurological outcomes. (A) The gamma band fractions over 15–30 min post-ROSC were significantly higher than the other subbands, including delta, theta, alpha, and beta band fractions ( $p < 0.05$ , respectively). (B and C) Strong and positive correlations were identified between gamma band power over 15–30 min post-ROSC and higher NDS ( $r_s = 0.705$ ,  $p = 0.027$ ,  $r_s = 0.693$ ,  $p = 0.031$ , and  $r_s = 0.614$ ,  $p = 0.064$ , respectively) and between gamma band fraction during the same period and better neurological outcomes ( $r_s = 0.796$ ,  $p = 0.008$ ,  $r_s = 0.912$ ,  $p < 0.001$ , and  $r_s = 0.669$ ,  $p = 0.04$ , respectively). EEG, electroencephalography; NDS, neurological deficit score; ROSC, return of spontaneous circulation. Data represent as mean  $\pm$  SD. Comparisons among temporal changes of EEG parameters were performed with repeated measures one-way ANOVA with Bonferroni correction; correlations between EEG parameters and NDS were performed with Spearman's correlation. \* $p < 0.05$ , \*\* $p < 0.01$ , \*\*\* $p < 0.001$ .

the ARAS must remain intact and contribute to the generation of gamma band oscillations for the brain to gain arousal and be conscious.<sup>48</sup> Here, we observed surged

gamma band activity in EEG during the hyperacute stage post-CA resuscitation, suggesting the function of the ARAS is intact, and the cerebral cortex could be aroused

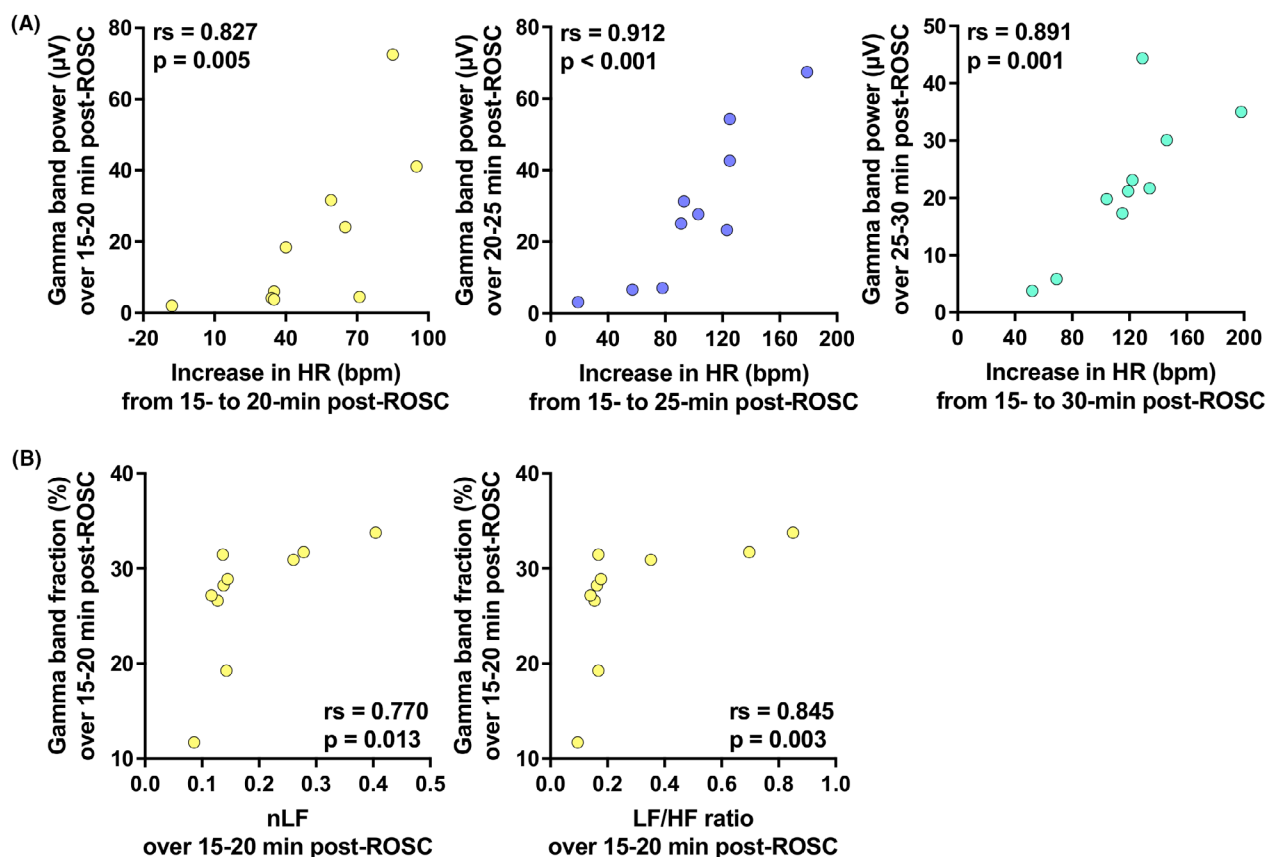


**Figure 6.** Correlations between changes in HR/HRV and dynamics of EEG signals during the hyperacute stage after resuscitation. (A) Very strong correlations were revealed between HR changes and gamma band power at 15–20 min ( $r_s = 0.827$ ,  $p = 0.005$ ), 20–25 min ( $r_s = 0.912$ ,  $p < 0.001$ ), and 25–30 min ( $r_s = 0.891$ ,  $p = 0.001$ ) post-ROSC. (B) Gamma band fraction over 15–20 min post-ROSC exhibited significant correlations with LF power ( $r_s = 0.770$ ,  $p = 0.013$ ) and LF/HF ratio ( $r_s = 0.845$ ,  $p = 0.003$ ). bpm, beats per minute; HR, heart rate; LF/HF, low frequency/high frequency; nLF, normalized low frequency; ROSC, return to spontaneous circulation. Correlations between HR/HRV parameters and EEG parameters were performed with Spearman's correlation.

and generate its own gamma band oscillations. These factors are critical for the recovery of arousal and awareness from CA-induced unresponsiveness.

Our findings also showed that a significant increase in HR over 15–30 min post-ROSC that corresponded to LF/HF ratio changes was correlated with better NDS. Notably, this increased HR was not significantly affected by the BT changes since a different dynamic pattern together with a weak correlation was detected in this study. A complex network of cortical and subcortical brain regions is involved in the central control of the cardiovascular function.<sup>10</sup> While noting the focus of this study, it has been suggested that the insular cortex plays an important role in regulating the heart–brain axis.<sup>49</sup> Electrical stimulation of the rostral posterior insula in rats exerted a tachycardia effect which could be abolished by atenolol, a  $\beta$ -blocker medication, indicating this effect was mediated by increased sympathetic activity.<sup>50</sup> In the awake brain, gamma oscillations require a sufficient

number of brain regions displaying gamma band activity to sustain the resonance.<sup>48</sup> During 15–30 min post-ROSC, the insular cortex may participate in generating the resonance of gamma band oscillations and simultaneously initiate the autonomic response at the cortical level. The strongly correlated HR and EEG activity augmentation suggests the role of autonomic recovery and an intact heart–brain interaction post-CA resuscitation.

Subcortical brain regions also contribute to the regulation of autonomic response after resuscitation. For instance, the cardiovascular responses induced by the insular cortex have been suggested to be relayed through the lateral hypothalamic area (LHA).<sup>49</sup> The LHA itself plays an important role in the coordination of diverse aspects of physiology and behavior, including stress, arousal, and autonomic function.<sup>51</sup> It is composed of a heterogeneous population of neurons, which contains orexinergic neurons.<sup>51</sup> Orexin neuropeptides are crucial

for maintaining a long period of arousal.<sup>52</sup> It was found that the orexin-induced depolarizing current could produce significant high frequency, including gamma, input to cholinergic neurons in the pedunculopontine nucleus (PPN).<sup>53</sup> Meanwhile, orexin neurons send projections to the rostral ventrolateral medulla (RVLM) and participate in regulating sympathetic tone.<sup>54</sup> Hence, it is possible that resuscitation-induced orexinergic neuron activation generates simultaneous responses in the PPN and the RVLM, leading to concurrent alterations in cardiac and cortical electrophysiological activity.

CA-induced cerebral damage could lead to impairment in autonomic function, shown as varied levels of cardiovascular dysfunction.<sup>10</sup> Dysregulation of the autonomic nervous system post-resuscitation is often associated with ECG changes, with various clinical manifestations ranging from mild and transient changes to severe and irreversible cardiac injury.<sup>10</sup> However, identification of these cardiovascular incidents post-CA in relation to the evaluation of neurological deficit as well as recovery remains challenging. The concurrent autonomic and cortical functional recovery observed in this study highlights the necessity of employing a multifaceted monitoring system during hyperacute management in CA patients. A comprehensive assessment of cortical neuronal activity together with autonomic responsiveness may provide a better understanding and estimation of the preservation of cardiovascular function after resuscitation, guiding our clinical practice to develop novel therapies and improve the implementation of current ones to improve outcomes.

Our study has limitations. First, the number of animals studied in this cohort was limited to 10. The responses of both survival and recovery post-ROSC, along with cortical and cardiac responses, were consistent in this cohort, justifying the small cohort. In previous work, however, we showed that a sample size of 10 was adequate to detect pathophysiological alterations post-resuscitation, and further, subgroups of five enabled us to detect the differential between good and poor neurological outcomes.<sup>25,27</sup> Second, we studied only male rats in this study. Male–female differences in survival and neurological outcomes after resuscitation from CA have been reported in clinical trials, and males appear to survive and recover better than females.<sup>55,56</sup> Preclinical research shows that sex hormones lead to male–female outcomes differences after the ischemic brain injury<sup>57,58</sup> and male–female differences in clinical electrophysiology and arrhythmias,<sup>59</sup> but how this male–female difference impacts autonomic response to resuscitation from CA remains largely unknown. The impact of male–female differences after resuscitation from CA is less established. Registry studies showed that males had better survival outcomes.<sup>56,60</sup> However, a systematic review found that the advantage of males in survival was

nullified after adjustment.<sup>55</sup> It is evident that the question of male–female in relation to outcomes after CA needs further investigation. This is a hypothesis that we intend to address in future studies. Third, we only evaluated the acute neurological outcome via NDS at 4-h post-ROSC. Our goal is to understand the hyperacute post-resuscitation recovery, but as a translational platform, this period is crucial for interventions that could possibly reverse neurologic injury. After this observation, we will extend the survival duration to evaluate the long-term consequences of autonomic recovery in subsequent studies in the future. Moreover, the underlying mechanism for the positive correlation between increased HR/sympathetic tone and enhanced EEG activity identified in this study has not been addressed. This correlation opens many considerations, while outside the scope of this study, and deserves more focused mechanistic investigation.

In conclusion, this study demonstrates that a significant hyperacute recovery in the autonomic function, manifested by an increase in HR and a correspondingly elevated sympathetic tone during the post-CA hyperacute stage, is associated with favorable functional outcomes. The increased HR and elevated sympathetic tone are strongly correlated with a remarkable recovery of EEG activity, presented by enhanced gamma band power. This coupled brain and heart electrophysiological arousal may indicate preserved heart–brain axis and autonomic responsiveness after resuscitation. While this observation needs further mechanistic validation, it presents a translational opportunity for better autonomic and neurologic monitoring during the early periods after CA that can potentially guide early management in post-resuscitation patients.

## Author Contributions

YG and PG designed and performed experiments. YG conducted data analysis. PA performed EEG and HRV analyses. RGG, NVT, SMC, and YG conceived this study. NVT and RGG supervised the project, coordinated the study, and secured the funding. All authors contributed to the manuscript revisions and approved for the final version.

## Acknowledgements

None.

## Funding Information

This work was supported by NIH grants R01 HL071568 (Nitish V. Thakor and Romergryko G. Geocadin) and R01 HL139158 (Nitish V. Thakor). Sung-min Cho is

funded by NIH grant K23 HL1157610 and Hyperfine Inc. (SAFE MRI ECMO study).

## Conflict of Interest

The authors declared that they have no conflicts of interest.

## References

1. Benjamin EJ, Muntner P, Alonso A, et al. Heart disease and stroke Statistics-2019 update a report from the American Heart Association. *Circulation*. 2019;139(10):E56-E528. doi:[10.1161/Cir.0000000000000659](https://doi.org/10.1161/Cir.0000000000000659)
2. Tsao CW, Aday AW, Almarzooq ZI, et al. Heart disease and stroke Statistics-2023 update: a report from the American Heart Association. *Circulation*. 2023;147(8):e93-e621. doi:[10.1161/CIR.0000000000001123](https://doi.org/10.1161/CIR.0000000000001123)
3. Nolan JP, Neumar RW, Adrie C, et al. Post-cardiac arrest syndrome: epidemiology, pathophysiology, treatment, and prognostication. A Scientific Statement from the International Liaison Committee on Resuscitation; the American Heart Association Emergency Cardiovascular Care Committee; the Council on Cardiovascular Surgery and Anesthesia; the Council on Cardiopulmonary, Perioperative, and Critical Care; the Council on Clinical Cardiology; the Council on Stroke. *Resuscitation*. 2008;79(3):350-379. doi:[10.1016/j.resuscitation.2008.09.017](https://doi.org/10.1016/j.resuscitation.2008.09.017)
4. Dragancea I, Rundgren M, Englund E, Friberg H, Cronberg T. The influence of induced hypothermia and delayed prognostication on the mode of death after cardiac arrest. *Resuscitation*. 2013;84(3):337-342. doi:[10.1016/j.resuscitation.2012.09.015](https://doi.org/10.1016/j.resuscitation.2012.09.015)
5. Mulder M, Gibbs HG, Smith SW, et al. Awakening and withdrawal of life-sustaining treatment in cardiac arrest survivors treated with therapeutic hypothermia. *Crit Care Med*. 2014;42(12):2493-2499. doi:[10.1097/Ccm.0000000000000540](https://doi.org/10.1097/Ccm.0000000000000540)
6. Geocadin RG, Callaway CW, Fink EL, et al. Standards for studies of neurological prognostication in comatose survivors of cardiac arrest: a scientific statement from the American Heart Association. *Circulation*. 2019;140(9):e517-e542. doi:[10.1161/CIR.0000000000000702](https://doi.org/10.1161/CIR.0000000000000702)
7. Busl KM, Greer DM. Hypoxic-ischemic brain injury: pathophysiology, neuropathology and mechanisms. *NeuroRehabilitation*. 2010;26(1):5-13. doi:[10.3233/NRE-2010-0531](https://doi.org/10.3233/NRE-2010-0531)
8. Kawai K, Nitecka L, Ruetzler CA, et al. Global cerebral ischemia associated with cardiac-arrest in the rat: 1. Dynamics of early neuronal changes. *J Cerebr Blood F Met*. 1992;12(2):238-249. doi:[10.1038/jcbfm.1992.34](https://doi.org/10.1038/jcbfm.1992.34)
9. Brisson CD, Hsieh YT, Kim D, Jin AY, Andrew RD. Brainstem neurons survive the identical ischemic stress that kills higher neurons: insight to the persistent vegetative state. *PloS One*. 2014;9(5):e96585. doi:[10.1371/journal.pone.0096585](https://doi.org/10.1371/journal.pone.0096585)
10. Tahsili-Fahadan P, Geocadin RG. Heart-brain axis effects of neurologic injury on cardiovascular function. *Circ Res*. 2017;120(3):559-572. doi:[10.1161/Circresaha.116.308446](https://doi.org/10.1161/Circresaha.116.308446)
11. Amorim E, Rittenberger JC, Baldwin ME, Callaway CW, Popescu A, Serv PCA. Malignant EEG patterns in cardiac arrest patients treated with targeted temperature management who survive to hospital discharge. *Resuscitation*. 2015;90:127-132. doi:[10.1016/j.resuscitation.2015.03.005](https://doi.org/10.1016/j.resuscitation.2015.03.005)
12. Mettenburg JM, Agarwal V, Baldwin M, Rittenberger JC. Discordant observation of brain injury by MRI and malignant electroencephalography patterns in comatose survivors of cardiac arrest following therapeutic hypothermia. *Am J Neuroradiol*. 2016;37(10):1787-1793. doi:[10.3174/ajnr.A4839](https://doi.org/10.3174/ajnr.A4839)
13. Andresen JM, Girard TD, Pandharipande PP, Davidson MA, Ely EW, Watson PL. Burst suppression on processed electroencephalography as a predictor of postcoma delirium in mechanically ventilated ICU patients. *Crit Care Med*. 2014;42(10):2244-2251. doi:[10.1097/Ccm.0000000000000522](https://doi.org/10.1097/Ccm.0000000000000522)
14. Sivaraju A, Gilmore EJ, Wira CR, et al. Prognostication of post-cardiac arrest coma: early clinical and electroencephalographic predictors of outcome. *Intens Care Med*. 2015;41(7):1264-1272. doi:[10.1007/s00134-015-3834-x](https://doi.org/10.1007/s00134-015-3834-x)
15. Hofmeijer J, Tjepkema-Cloostermans MC, van Putten MJAM. Burst-suppression with identical bursts: a distinct EEG pattern with poor outcome in postanoxic coma. *Clin Neurophysiol*. 2014;125(5):947-954. doi:[10.1016/j.clinph.2013.10.017](https://doi.org/10.1016/j.clinph.2013.10.017)
16. Geocadin RG, Sherman DL, Christian Hansen H, et al. Neurological recovery by EEG bursting after resuscitation from cardiac arrest in rats. *Resuscitation*. 2002;55(2):193-200. doi:[10.1016/s0300-9572\(02\)00196-x](https://doi.org/10.1016/s0300-9572(02)00196-x)
17. Tong S, Bezerianos A, Paul J, Zhu Y, Thakor N. Nonextensive entropy measure of EEG following brain injury from cardiac arrest. *Physica A*. 2002;305(3-4):619-628. doi:[10.1016/S0378-4371\(01\)00621-5](https://doi.org/10.1016/S0378-4371(01)00621-5)
18. Shaffer F, Ginsberg JP. An overview of heart rate variability metrics and norms. *Front Public Health*. 2017;5:258. doi:[10.3389/fpubh.2017.00258](https://doi.org/10.3389/fpubh.2017.00258)
19. Thomsen JH, Hassager C, Bro-Jeppesen J, et al. Sinus bradycardia during hypothermia in comatose survivors of out-of-hospital cardiac arrest - a new early marker of favorable outcome? *Resuscitation*. 2015;89:36-42. doi:[10.1016/j.resuscitation.2014.12.031](https://doi.org/10.1016/j.resuscitation.2014.12.031)
20. Boardman A, Schlindwein FS, Thakor NV, Kimura T, Geocadin RG. Detection of asphyxia using heart rate variability. *Med Biol Eng Comput*. 2002;40(6):618-624. doi:[10.1007/BF02345299](https://doi.org/10.1007/BF02345299)



21. Goldstein B, Fiser DH, Kelly MM, Mickelsen D, Ruttimann U, Pollack MM. Decomplexification in critical illness and injury: relationship between heart rate variability, severity of illness, and outcome. *Crit Care Med*. 1998;26(2):352-357. doi:[10.1097/00003246-199802000-00040](https://doi.org/10.1097/00003246-199802000-00040)
22. Dekker JM, Crow RS, Folsom AR, et al. Low heart rate variability in a 2-minute rhythm strip predicts risk of coronary heart disease and mortality from several causes: the ARIC study. Atherosclerosis risk in communities. *Circulation*. 2000;102(11):1239-1244. doi:[10.1161/01.cir.102.11.1239](https://doi.org/10.1161/01.cir.102.11.1239)
23. Chen WL, Tsai TH, Huang CC, Chen JH, Kuo CD. Heart rate variability predicts short-term outcome for successfully resuscitated patients with out-of-hospital cardiac arrest. *Resuscitation*. 2009;80(10):1114-1118. doi:[10.1016/j.resuscitation.2009.06.020](https://doi.org/10.1016/j.resuscitation.2009.06.020)
24. Geocadin RG, Muthuswamy J, Sherman DL, Thakor NV, Hanley DF. Early electrophysiological and histologic changes after global cerebral ischemia in rats. *Mov Disord*. 2000;15(Suppl 1):14-21. doi:[10.1002/mds.870150704](https://doi.org/10.1002/mds.870150704)
25. Guo Y, Cho SM, Wei Z, et al. Early thalamocortical reperfusion leads to neurologic recovery in a rodent cardiac arrest model. *Neurocrit Care*. 2022;37(1):60-72. doi:[10.1007/s12028-021-01432-9](https://doi.org/10.1007/s12028-021-01432-9)
26. Katz L, Ebmeyer U, Safar P, Radovsky A, Neumar R. Outcome model of asphyxial cardiac arrest in rats. *J Cereb Blood Flow Metab*. 1995;15(6):1032-1039. doi:[10.1038/jcbfm.1995.129](https://doi.org/10.1038/jcbfm.1995.129)
27. Wei Z, Wang Q, Modi HR, et al. Acute-stage MRI cerebral oxygen consumption biomarkers predict 24-hour neurological outcome in a rat cardiac arrest model. *NMR Biomed*. 2020;33(11):e4377. doi:[10.1002/nbm.4377](https://doi.org/10.1002/nbm.4377)
28. Akselrod S, Gordon D, Ubel FA, Shannon DC, Barger AC, Cohen RJ. Power Spectrum analysis of heart-rate fluctuation - a quantitative probe of beat-to-beat cardiovascular control. *Science*. 1981;213(4504):220-222. doi:[10.1126/science.6166045](https://doi.org/10.1126/science.6166045)
29. Eckberg DL. Sympathovagal balance - a critical appraisal. *Circulation*. 1997;96(9):3224-3232. doi:[10.1161/01.Cir.96.9.3224](https://doi.org/10.1161/01.Cir.96.9.3224)
30. Sherman DL, Williams A, Gd S, et al. Intranasal orexin after cardiac arrest leads to increased electroencephalographic gamma activity and enhanced neurologic recovery in rats. *Crit Care Explor*. 2021;3(2):e0349. doi:[10.1097/CCE.0000000000000349](https://doi.org/10.1097/CCE.0000000000000349)
31. Tong SB, Bezerianos A, Malhotra A, Zhu YS, Thakor N. Parameterized entropy analysis of EEG following hypoxic-ischemic brain injury. *Phys Lett A*. 2003;314(5-6):354-361. doi:[10.1016/S0375-9601\(03\)00949-6](https://doi.org/10.1016/S0375-9601(03)00949-6)
32. Bezerianos A, Tong S, Thakor N. Time-dependent entropy estimation of EEG rhythm changes following brain ischemia. *Ann Biomed Eng*. 2003;31(2):221-232. doi:[10.1114/1.1541013](https://doi.org/10.1114/1.1541013)
33. Koenig MA, Jia X, Kang X, Velasquez A, Thakor NV, Geocadin RG. Intraventricular orexin-a improves arousal and early EEG entropy in rats after cardiac arrest. *Brain Res*. 2009;1255:153-161. doi:[10.1016/j.brainres.2008.11.102](https://doi.org/10.1016/j.brainres.2008.11.102)
34. Modi HR, Wang Q, Gd S, et al. Intranasal post-cardiac arrest treatment with orexin-a facilitates arousal from coma and ameliorates neuroinflammation. *PloS One*. 2017;12(9):e0182707. doi:[10.1371/journal.pone.0182707](https://doi.org/10.1371/journal.pone.0182707)
35. Shin HC, Tong S, Yamashita S, Jia X, Geocadin RG, Thakor NV. Quantitative EEG and effect of hypothermia on brain recovery after cardiac arrest. *IEEE Trans Biomed Eng*. 2006;53(6):1016-1023. doi:[10.1109/TBME.2006.873394](https://doi.org/10.1109/TBME.2006.873394)
36. Geocadin RG, Ghodadra R, Kimura T, et al. A novel quantitative EEG injury measure of global cerebral ischemia. *Clin Neurophysiol*. 2000;111(10):1779-1787. doi:[10.1016/S1388-2457\(00\)00379-5](https://doi.org/10.1016/S1388-2457(00)00379-5)
37. Pulsinelli WA, Brierley JB, Plum F. Temporal profile of neuronal damage in a model of transient forebrain ischemia. *Ann Neurol*. 1982;11(5):491-498. doi:[10.1002/ana.410110509](https://doi.org/10.1002/ana.410110509)
38. Milani-Nejad N, Janssen PM. Small and large animal models in cardiac contraction research: advantages and disadvantages. *Pharmacol Ther*. 2014;141(3):235-249. doi:[10.1016/j.pharmthera.2013.10.007](https://doi.org/10.1016/j.pharmthera.2013.10.007)
39. Gu X, Simons FE, Simons KJ. Epinephrine absorption after different routes of administration in an animal model. *Biopharm Drug Dispos*. 1999;20(8):401-405. doi:[10.1002/1099-081x\(199911\)20:8<401::aid-bdd204>3.0.co;23C401-I](https://doi.org/10.1002/1099-081x(199911)20:8<401::aid-bdd204>3.0.co;23C401-I)
40. Maloney KJ, Cape EG, Gotman J, Jones BE. High-frequency gamma electroencephalogram activity in association with sleep-wake states and spontaneous behavior/familyNames in the rat. *Neuroscience*. 1997;76(2):541-555. doi:[10.1016/S0306-4522\(96\)00298-9](https://doi.org/10.1016/S0306-4522(96)00298-9)
41. Mileykovskiy BY, Kiyashchenko LI, Siegel JM. Behavioral correlates of activity in identified hypocretin/orexin neurons. *Neuron*. 2005;46(5):787-798. doi:[10.1016/j.neuron.2005.04.035](https://doi.org/10.1016/j.neuron.2005.04.035)
42. Hoesch RE, Koenig MA, Geocadin RG. Coma after global ischemic brain injury: pathophysiology and emerging therapies. *Crit Care Clin*. 2008;24(1):25-44, vii-viii. doi:[10.1016/j.ccc.2007.11.003](https://doi.org/10.1016/j.ccc.2007.11.003)
43. Koenig MA, Kaplan PW, Thakor NV. Clinical neurophysiologic monitoring and brain injury from cardiac arrest. *Neurol Clin*. 2006;24(1):89-106. doi:[10.1016/j.ncl.2005.11.003](https://doi.org/10.1016/j.ncl.2005.11.003)
44. Young GB. The EEG in coma. *J Clin Neurophysiol*. 2000;17(5):473-485. doi:[10.1097/00004691-200009000-00006](https://doi.org/10.1097/00004691-200009000-00006)
45. Thakor NV, Tong S. Advances in quantitative electroencephalogram analysis methods. *Annu Rev Biomed Eng*. 2004;6:453-495. doi:[10.1146/annurev.bioeng.5.040202.121601](https://doi.org/10.1146/annurev.bioeng.5.040202.121601)



46. Cha KM, Thakor NV, Shin HC. Novel early EEG measures predicting brain recovery after cardiac arrest. *Entropy-Switz*. 2017;19(9):466. doi:[10.3390/e19090466](https://doi.org/10.3390/e19090466)
47. Edlow BL, Takahashi E, Wu ON, et al. Neuroanatomic connectivity of the human ascending arousal system critical to consciousness and its disorders. *J Neuropath Exp Neur*. 2012;71(6):531-546. doi:[10.1097/NEN.0b013e3182588293](https://doi.org/10.1097/NEN.0b013e3182588293)
48. Garcia-Rill E, Kezunovic N, Hyde J, Simon C, Beck P, Urbano FJ. Coherence and frequency in the reticular activating system (RAS). *Sleep Med Rev*. 2013;17(3):227-238. doi:[10.1016/j.smrv.2012.06.002](https://doi.org/10.1016/j.smrv.2012.06.002)
49. Verberne AJ, Owens NC. Cortical modulation of the cardiovascular system. *Prog Neurobiol*. 1998;54(2):149-168. doi:[10.1016/s0301-0082\(97\)00056-7](https://doi.org/10.1016/s0301-0082(97)00056-7)
50. Oppenheimer SM, Cechetto DF. Cardiac chronotropic organization of the rat insular cortex. *Brain Res*. 1990;533(1):66-72. doi:[10.1016/0006-8993\(90\)91796-j](https://doi.org/10.1016/0006-8993(90)91796-j)
51. Bonnavion P, Mickelsen LE, Fujita A, de Lecea L, Jackson AC. Hubs and spokes of the lateral hypothalamus: cell types, circuits and behaviour. *J Physiol*. 2016;594(22):6443-6462. doi:[10.1113/JP271946](https://doi.org/10.1113/JP271946)
52. Scammell TE, Arrigoni E, Lipton JO. Neural circuitry of wakefulness and sleep. *Neuron*. 2017;93(4):747-765. doi:[10.1016/j.neuron.2017.01.014](https://doi.org/10.1016/j.neuron.2017.01.014)
53. Ishibashi M, Gumenchuk I, Kang B, et al. Orexin receptor activation generates gamma band input to cholinergic and serotonergic arousal system neurons and drives an intrinsic  $Ca^{2+}$ -dependent resonance in LDT and PPT cholinergic neurons. *Front Neurol*. 2015;6:120. doi:[10.3389/fneur.2015.00120](https://doi.org/10.3389/fneur.2015.00120)
54. Grimaldi D, Silvani A, Benarroch EE, Cortelli P. Orexin/hypocretin system and autonomic control: new insights and clinical correlations. *Neurology*. 2014;82(3):271-278. doi:[10.1212/WNL.0000000000000045](https://doi.org/10.1212/WNL.0000000000000045)
55. Lei H, Hu J, Liu L, Xu D. Sex differences in survival after out-of-hospital cardiac arrest: a meta-analysis. *Crit Care*. 2020;24(1):613. doi:[10.1186/s13054-020-03331-5](https://doi.org/10.1186/s13054-020-03331-5)
56. Nehme Z, Andrew E, Bernard S, Smith K. Sex differences in the quality-of-life and functional outcome of cardiac arrest survivors. *Resuscitation*. 2019;137:21-28. doi:[10.1016/j.resuscitation.2019.01.034](https://doi.org/10.1016/j.resuscitation.2019.01.034)
57. Haast RA, Gustafson DR, Kiliaan AJ. Sex differences in stroke. *J Cereb Blood Flow Metab*. 2012;32(12):2100-2107. doi:[10.1038/jcbfm.2012.141](https://doi.org/10.1038/jcbfm.2012.141)
58. Chauhan A, Moser H, McCullough LD. Sex differences in ischaemic stroke: potential cellular mechanisms. *Clin Sci (Lond)*. 2017;131(7):533-552. doi:[10.1042/CS20160841](https://doi.org/10.1042/CS20160841)
59. Tadros R, Ton AT, Fiset C, Nattel S. Sex differences in cardiac electrophysiology and clinical arrhythmias: epidemiology, therapeutics, and mechanisms. *Can J Cardiol*. 2014;30(7):783-792. doi:[10.1016/j.cjca.2014.03.032](https://doi.org/10.1016/j.cjca.2014.03.032)
60. Kotini-Shah P, Del Rios M, Khosla S, et al. Sex differences in outcomes for out-of-hospital cardiac arrest in the United States. *Resuscitation*. 2021;163:6-13. doi:[10.1016/j.resuscitation.2021.03.020](https://doi.org/10.1016/j.resuscitation.2021.03.020)

## Supporting Information

Additional supporting information may be found online in the Supporting Information section at the end of the article.

### Appendix S1.